Check for updates

ChemFoodChem

ChemFoodChem
Chemistry Europe
European Chemical Societies Publishing

RESEARCH ARTICLE OPEN ACCESS

Mechanical Characterization of Acidic Casein Gels From Micellar Casein Powder: Influence of Lactose and Sucrose

Ronald Gebhardt | Thomas Pütz

Chair of Soft Matter Process Engineering (AVT.SMP), RWTH Aachen University, Aachen, Germany

Correspondence: Ronald Gebhardt (ronald.gebhardt@avt.rwth-aachen.de)

Received: 5 December 2025 | **Revised:** 16 March 2026 | **Accepted:** 19 March 2026

Keywords: acidic casein gels | force-displacement curves | micellar casein powder | sugar–protein interactions | system dynamics simulation

ABSTRACT

This study compared the effects of lactose and sucrose at concentrations of 2%–14% (*w*/*w*) on acidic casein gels. Lactose significantly compacted casein gel microstructure, whereas sucrose induced minimal changes. All gels exhibited two-phase linear force–displacement curves, with increasing slopes as the sugar concentration increased, more markedly for lactose. For both sugars, a local force peak was observed at concentrations above 6%. The peak shifted to lower displacements and increased in intensity with concentration, more pronounced for lactose. The sugar-induced force peaks could be separated by simultaneously fitting our previously developed gel network model to the force curves and their first derivatives. System dynamics analysis revealed that this peak arises from weak sugar–protein bonds. The viscous network delays the build-up and release of the tension in these bonds by about 4.3 s. Higher lactose concentrations form more bonds, stiffening the gel and accelerating tension development. Consequently, the force peak occurs at lower displacements and the bonds rupture earlier. These results show that sugars can selectively enhance protein interactions in casein gels and that the resulting sugar-induced force peaks serve as mechanical probes for investigating viscoelastic network dynamics, which has implications for sugar-modified milk gels and protein-based functional materials.

1 | Introduction

Food biopolymers have several advantages over synthetic materials, including their renewable origin, low cost, biocompatibility, and biodegradability. The gels formed from these biopolymers now offer a comparable range of applications and performance [1]. The polymers can be obtained from complex biofluids such as milk, which, in addition to a fat phase and the main proteinogenic components, also contains low-molecular-weight carbohydrates such as lactose [2]. The main protein component, casein, can be used to produce gelled food structures and novel materials such as fibers and microparticles [3–5]. Caseins are present in milk in the form of association colloids, known as casein micelles [6]. These are composed of the four main caseins (α_{S1}–, α_{S1}–, β– and κ–casein), which are cross-linked via hydrophobic interactions and colloidal calcium phosphate [7, 8]. A κ-casein surface layer forms a steric barrier on their surface, preventing uncontrolled aggregation [9]. If this surface layer is destabilized—as in this study by acidification—the micelles lose their colloidal stability, leading to aggregation of the casein micelles and ultimately to the formation of a protein particle gel [10]. When acidification is applied to heated milk, the presence of denatured whey proteins reduces surface repulsion, promoting the formation of additional protein aggregates via disulfide bonds. This shifts gel formation to a higher pH, resulting in stiffer acidic gels than those formed from unheated milk [11]. Similar effects caused by denatured whey proteins must also be taken into account in the case of thermally pretreated micellar casein powders (MC–powder), which are preferred as raw material for analytical studies on casein gel systems and for the

This is an open access article under the terms of the Creative Commons Attribution License, which permits use, distribution and reproduction in any medium, provided the original work is properly cited.

© 2026 The Author(s). *ChemFoodChem* published by Chemistry Europe and Wiley-VCH GmbH.

production of new functional structures. MC–powders offer a standardized protein composition, extended shelf life and enable precise adjustment of the protein concentration in reconstituted milk systems, while maintaining the structural and functional integrity of native casein micelles [12]. During rehydration, the viscoelastic and mechanical properties are also retained, resulting in casein gels with reproducible microstructure and network behavior [13]. Based on MC–powders, for example, microparticles with controlled swelling capacity and stability were produced that remained stable as biocompatible carriers in the gastrointestinal tract or released active substances in the tissue [14–16].

Low-molecular-weight sugars are common food additives that can affect the functionality of proteins. This occurs either through noncovalent physical interactions, such as hydrogen bonding and osmotic effects, or through covalent chemical modifications, such as glycation via the Maillard reaction [17]. Some studies have investigated the effect of lactose and sucrose on the structure and interactions of milk proteins. Sánchez-García et al. showed that whey proteins modulate the crystallization of lactose, with the effect being highly dependent on pH and more pronounced at neutral pH than at acidic pH [18]. Vega and Roos also showed that caseins delay the crystallization rates of lactose more than those of sucrose. They attributed these differences to interactions between proteins, sugars, and water, and suggested hydrogen bonds between the hydrophilic groups of caseins and the hydroxyl groups of sugars as a possible mechanism [19]. Mozersky et al. observed that the addition of ∼10% lactose decreased the apparent micellar protein mass of reconstituted casein micelles. This value was determined from sedimentation field-flow fractionation elution profiles, which were converted from retention time to apparent protein mass using hydrodynamic theory [20]. In contrast, sucrose had only a minor effect. Since both sugars were tested in equimolar concentrations and thus exert comparable osmotic pressure, the observed effect of lactose on micelle size suggests a more specific mechanism. Furthermore, it has been demonstrated that sucrose can influence caseinate self-assembly by promoting hydrogen bonding and protein dehydration. This enhances the interconnectivity of aggregates and improves the viscoelasticity and homogeneity of acid-induced gels [21]. However, only subtle changes in gel microstructure have been reported in confocal imaging at sucrose levels up to about 15% (*w*/*v*), suggesting that structural effects remain modest within this concentration range [22]. In contrast, the presence of lactose in MC–powder-based acid gels within comparable concentration ranges resulted in a significantly more compact and less porous gel network than the sugar-free samples [23].

However, sugars typically also increase the viscosity of aqueous solutions, with only minor differences between lactose and sucrose solutions [24]. In general, an increase in viscosity can influence force–displacement curves, as microintubation experiments on biological hydrogels have shown [25]. Such force–displacement curves are typically used to characterize protein and polymer gels, whereby linear increases and maxima are evaluated to determine elasticity and compressive strength. AFM single-molecule studies on proteins have shown that force–elongation curves in such measurements exhibit characteristic sawtooth peaks, which can be attributed to the successive breaking of noncovalent interactions within the molecular structure [26].

Since MC powder preparations contain whey proteins that are already partially denatured due to industrial heat treatment during processing and spray drying, moderate heating below the typical denaturation temperature of ≤70°C can induce limited thiol-mediated cross-linking of whey proteins with casein micelles [27]. However, controlled pretreatment at 70°C produces pressure-stable and more elastic gel networks, which allows specific sugar-induced effects to be investigated. The constant temperature of the pretreatment ensures that the proportion of disulfide-reinforced contacts remains unchanged across all samples.

In this study, we compare the effect of lactose and sucrose on the force–displacement curves. We validate our gel network model and transfer the force–displacement data to the time domain in order to analyze the viscoelastic reactions of the network using system dynamics. This enables the mechanisms of sugar–protein interactions to be investigated, providing the basis for strategies to specifically adjust the stiffness and stability of soft casein networks using low-molecular-weight sugars.

2 | Experimental Section

2.1 | Chemicals

Micellar casein powder MC88 (MILEI GmbH, Germany) was used for preparing the suspensions. Lactose and sucrose were obtained from VWR (VWR International GmbH, Darmstadt, Germany), and glucono-delta-lactone (GDL) was purchased from Thermo Fisher (Thermo Fisher, USA). Simulated milk ultrafiltrate (SMUF) was prepared following the composition described by Dumpler [28]. All salts used for the SMUF solution were of analytical grade. To prevent microbial growth, sodium azide (Carl Roth GmbH + Co. KG, Germany) was added at a concentration of 0.5 g/L.

2.2 | Preparation of Casein Suspensions

Lactose or sucrose were dissolved in SMUF under moderate stirring. For high lactose concentrations, the solution was heated to 35°C while stirring and subsequently cooled to room temperature. MC88 was then added to achieve a final casein concentration of 5% (*w*/*w*). The mixture was stirred for 1 h at room temperature, for 16 h at 4°C, and again for 1 h at 37°C. To ensure complete hydration of the casein micelles and to ensure a homogeneous gel was obtained at the end, the suspension was then gently stirred at 30°C for 24 h. To determine the degree of hydration of the micellar casein during the rehydration process, the dispersions were subjected to light centrifugation (100 × *g*, 10 min, 20°C), and the total solids content of the supernatant was determined using the moisture analyzer Sartorius MA 37 (Sartorius AG, Göttingen, Germany). The measured amounts of solids were compared with the dry matter originally added to evaluate the recovery of the soluble material, which corresponded to the dry matter originally added.

25109936, 2026, 2, Downloaded from https://chemistry-europe.onlinelibrary.wiley.com/doi/10.1002/cfch.202500049 by Universitatsbibliothek RWTH Aachen University, Wiley Online Library on [10/06/2026]. See the Terms and Conditions (https://onlinelibrary.wiley.com/terms-and-conditions) on Wiley Online Library for rules of use; OA articles are governed by the applicable Creative Commons License

2.3 | Preparation of Acid Gels

To induce β-lactoglobulin denaturation, the solution was heated to 70°C for 11 min and then cooled in ice water for 10 min. GDL was added at a ratio of 0.5 g per g casein to initiate gelation. The mixture was stored at room temperature for approximately 20 h before testing. The final pH of the casein gels was 4.1 ± 0.2.

2.4 | Confocal Fluorescence Microscopy

After GDL addition, the samples were stained with Rhodamine B (Sigma-Aldrich, Saint Louis, MO, USA) by adding 1 mL of a 2 mM Rhodamine B solution prepared in SMUF. Glass slides were then coated with 200 µL of the casein solution and left at room temperature for gelation, which took approximately 20 h. To minimize evaporation, the slides were stored in a closed container with elevated humidity. Confocal images were acquired with an LSM 980 Airyscan 2 microscope (Carl Zeiss Microscopy GmbH, Jena, Germany) using excitation at 545 nm and emission at 566 nm.

2.5 | Mechanical Tests

Deformation experiments were conducted using a texture analyzer AGS-X (Shimadzu, Japan). After GDL addition and brief stirring, 20 g of the liquid casein solution was gently poured into 50 mL glass beakers with 4.2 cm in diameter. A circular plunger with a diameter of 12.7 mm penetrated the gels, and a force–distance curve was recorded at a crosshead speed of 0.1 mm s^{-1}. All measurements were performed at room temperature in at least technical triplicates.

2.6 | Modeling of Force–Displacement Curves

A four-parameter model was used to analyze the force–displacement curves ($F(d)$) in the elastic–plastic range before the maximum load was reached [27]. This connects two linear ranges with slopes k_1 and k_2 via a transition function, TF:

$$F(d) = k_1 \cdot d + (k_2 - k_1) \cdot (d - d^*) \cdot TF \tag{1}$$

where d is the displacement, d^* is the transition displacement at which the slope changes from k_1 to k_2, and k_T determines the steepness of the transition function, TF. The transition function is given by:

$$TF = \frac{1}{1 + e^{-k_T \cdot (d - d^*)}} \tag{2}$$

For $d \ll d^*$, the first linear component dominates since TF→0; for $d \gg d^*$, however, it is the second linear component that determines the curve. The original adjustment to the measured force values (rather than pressure) was performed using nonlinear regression. To more precisely determine the model parameters k_1, k_2, k_T, and d^*, the first derivative of the data $dF/d(d)$ was additionally fitted simultaneously with the analytical derivative of the model:

$$\frac{dF}{dd} = k_1 + (k_2 - k_1)\left(\frac{1}{1 + e^{-k_T \cdot (d - d^*)}} + (d - d^*)\frac{k_T \cdot e^{-k_T \cdot (d - d^*)}}{\left(1 + e^{-k_T \cdot (d - d^*)}\right)^2}\right) \tag{3}$$

Simultaneously adjusting force and derivative allows for more robust modeling. Evaluation was performed using the nonlinear fit routine in SigmaPlot (Systat Software, San Jose, CA, USA). A system dynamics model using Stella Professional (version 1.6; isee systems) was used to analyze the isolated force peaks. The time–integrated force curves were simulated with the Euler integration method and a temporal resolution of 0.025 s (DT = 1/40).

3 | Results and Discussion

Acidic gels made from MC–powder exhibit significantly reduced porosity upon the addition of lactose [23]. We observe a similar effect with our preparations. Figure 1 shows confocal fluorescence images of a gel sample without sugar and with 10% lactose and 10% sucrose. The sample without sugar shows strands in the sub-µm range that form a loose, homogeneous, and porous network. No significant changes are visible when 10% sucrose is added, while 10% lactose led to extensive areas with increased fluorescence intensity. These regions correspond to locally denser strands within the network, resulting in a significant reduction in porosity in these areas without whey leaking out of the gel as a whole. The observed differences in microstructure suggest that the compaction of the network could also influence the mechanical properties of the gels, in particular their compressive strength.

The acidic micellar casein gels were mechanically characterized using force–penetration experiments, whereby the indenter was pressed into the sample at a constant speed. In previous experiments, we demonstrated that the force–displacement curves consist of two successive linear increases in force before reaching the maximum [27].

After adding lactose and sucrose, we now observed for the first time a peak in the area of the second rise marked with dashed lines in Figure 2a,b. The force–displacement curves of gels with three selected concentrations of sugar are shown, illustrating that the peak becomes more pronounced and shifts to smaller penetration depths as the sugar concentration increases. It is also evident that both the first and second linear slope increased with rising sugar concentrations, with the increase being more pronounced in the case of lactose.

To analyze the sugar peak in detail, the background of the curves must first be subtracted as accurately as possible.

3.1 | Stable Modeling of the Sugar-Free Curve Using Simultaneous Fitting of the Force Curve and Derivative

Figure 3 shows a representative force–displacement curve for an acidic casein gel free of sugar. In line with our previous results, a two-stage, linear, progressive curve is consistently observed within the range of small penetration depths (up

25109936, 2026, 2, Downloaded from https://chemistry-europe.onlinelibrary.wiley.com/doi/10.1002/cfch.202500049 by Universitatsbibliothek RWTH Aachen University, Wiley Online Library on [10/06/2026]. See the Terms and Conditions (https://onlinelibrary.wiley.com/terms-and-conditions) on Wiley Online Library for rules of use; OA articles are governed by the applicable Creative Commons License

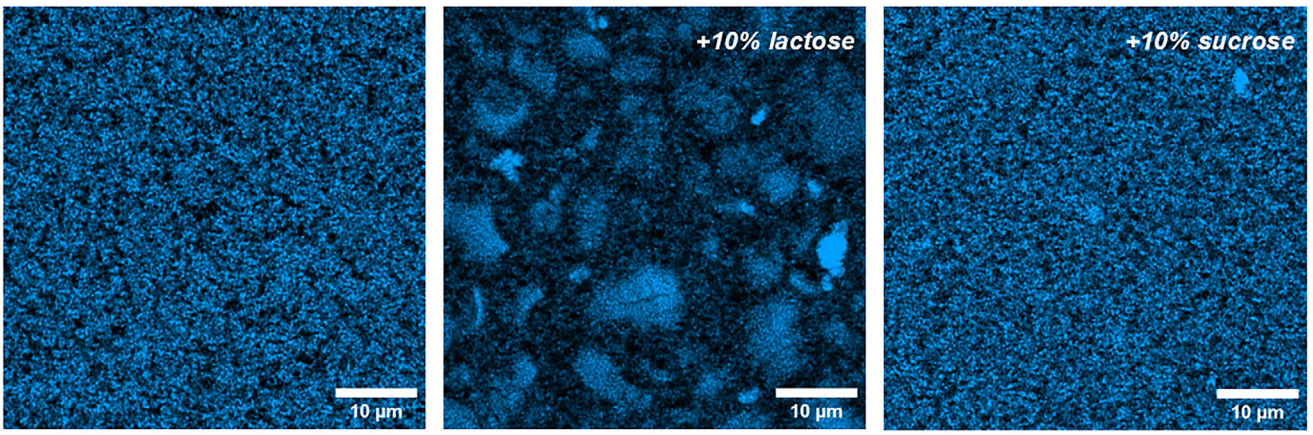


FIGURE 1 | Confocal fluorescence images of acidic casein gels prepared from MC–powder without sugar, with 10% lactose, and with 10% sucrose.

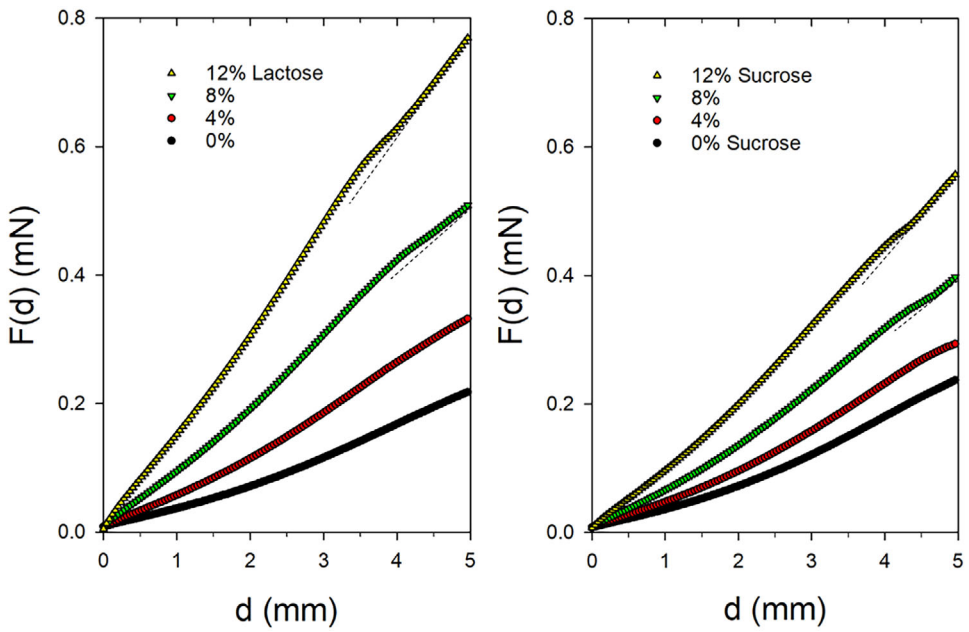


FIGURE 2 | Force–displacement curves of acidic casein gels containing various amounts of lactose (left) and sucrose (right). Force enhancement occurs in the second linear region (marked by the dashed lines), and this is more pronounced the higher the sugar concentration.

to approximately 5 mm). While the force signal is reversible at very small penetration depths (<1.5 mm), indicating primarily elastic response behavior of the gel, reversibility disappears within the range of the second linear increase (up to approximately 5 mm), suggesting the onset of plastic deformation.

At greater penetration depths, the reproducibility of the curve decreases; in some cases, a force maximum is reached immediately, whereas in others, as shown in Figure 3, the curve first flattens out before reaching a maximum. At even greater penetration depths, the force signal typically breaks down, indicating structural destruction of the gel. Later on, a renewed, steep increase in force can be observed, presumably due to increasing compaction of the gel in the sample container. As shown in our earlier work [27], the range below the maximum force, which encompasses elastic and plastic deformation, can be described using a model that couples the two linear increase ranges via a transition function (Equations 1 and 2). However, fitting individual force–displacement curves proves inaccurate and statistically insignificant, as illustrated by the adjustment in Figure S1 and the infinit′e standard errors in Table 1. In our previous study, we achieved credible and stable fit results by analyzing several curves simultaneously from gels with different thiol blocker concentrations [27].

To reliably describe individual curves, we have adopted a similar simultaneous fitting approach. This involves fitting not only the force–displacement function, but also its first derivative. As shown in the inset of Figure 3, the model precisely describes both the force–displacement function and its first derivative, with relative errors of less than 1% for k_1 and k_2, and less than 6% for d^* and k_T (see Table 1).

25109936, 2026, 2, Downloaded from https://chemistry-europe.onlinelibrary.wiley.com/doi/10.1002/cfch.202500049 by Universitatsbibliothek RWTH Aachen University, Wiley Online Library on [10/06/2026]. See the Terms and Conditions (https://onlinelibrary.wiley.com/terms-and-conditions) on Wiley Online Library for rules of use; OA articles are governed by the applicable Creative Commons License

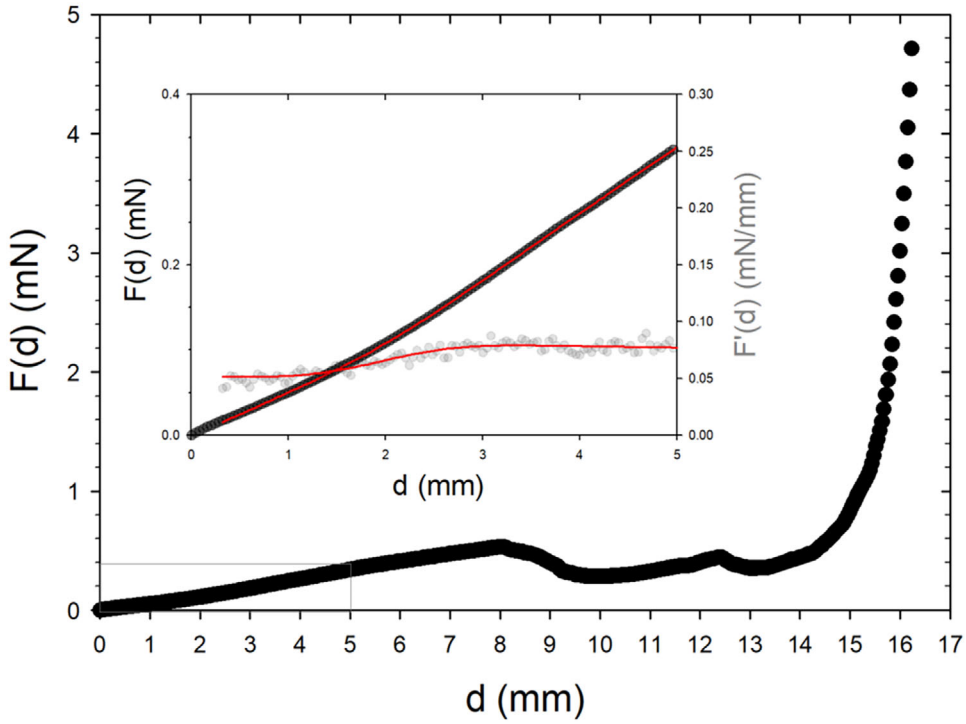


FIGURE 3 | A representative force–displacement curve for an acidic micellar casein gel is shown. Up to a penetration depth of 5 mm, a two-stage, linear, progressive curve can be observed which can be described by a transition model according to Pütz and Gebhardt [27]. Simultaneously fitting the original data and its first derivative, as shown in the inset, is a novel approach that provides stable and significant parameters with low error values.

TABLE 1 | Fit parameters for the sugar-free gel: Single vs. simultaneous fit.

Parameter	Fit to $f(x)$ value	Std. error	Joint fit to $f(x), f'(x)$ value	Std. error	Rel. error (%)
k_1 (mN·s^{-1})	0.06	∞	0.0538	0.0003	0.56
k_2 (mN·s^{-1})	0.09	∞	0.0769	0.0002	0.26
d^* (mm)	3	∞	1.967	0.030	1.5
k_T (mm^{-1})	1.7	∞	1.72	0.09	5.4

3.2 | Changes in Slopes and Transition Dynamics Due to Sugar

In order to analyze the effect of sugar on the force curves and extract the observed sugar peak, the mean force–displacement curves (mean from three repetitions) of gels with added lactose or sucrose were analyzed. For this purpose, eight gel preparations with sugar concentrations between 2% and 14% in 2% increments were produced and mechanically measured, and the resulting data were evaluated using a segmented simultaneous fit of the curve and its derivative (restricted to the pre- and post-peak regions). The procedure and the quality of the background subtraction are shown in Figure S2 and Table S1.

The resulting fits are statistically significant and show only minor relative errors in the four fit parameter values, as shown by the standard deviations of the fit parameters for the 5% and 12% sugar concentrations (calculated from the individual measurements) in Figure 4. The slopes of the two linear ranges (k_1 and k_2) show a slightly disproportionate increase with increasing sugar concentration. This can be explained by the osmotic effect of the sugar, which leads to dehydration of the caseins in the gel strands. This causes the caseins to interact more strongly with each other, resulting in more elastic gels. However, at higher sugar concentrations, the distinct differences in elasticity observed between lactose- and sucrose-containing gels cannot be accounted for by osmotic effects alone, as these are determined solely by the number of sugar molecules. At concentrations above 6%, a significantly stronger effect is observed for lactose: at 10% sugar addition, k_1 for the gels with lactose is about 40% and k_2 about 25% above the corresponding values for sucrose. Recent work also shows that an increase in the viscosity of the continuous phase generally leads to additional resistance during indentation, which can manifest itself in an increased slope of the force–displacement curve [25]. However, since the viscosities of the lactose and sucrose solutions examined are almost identical at the concentrations used [24], such a viscosity-related contribution can only represent a uniform base effect in

25109936, 2026, 2, Downloaded from https://chemistry-europe.onlinelibrary.wiley.com/doi/10.1002/cfch.202500049 by Universitatsbibliothek RWTH Aachen University, Wiley Online Library on [10/06/2026]. See the Terms and Conditions (https://onlinelibrary.wiley.com/terms-and-conditions) on Wiley Online Library for rules of use; OA articles are governed by the applicable Creative Commons License

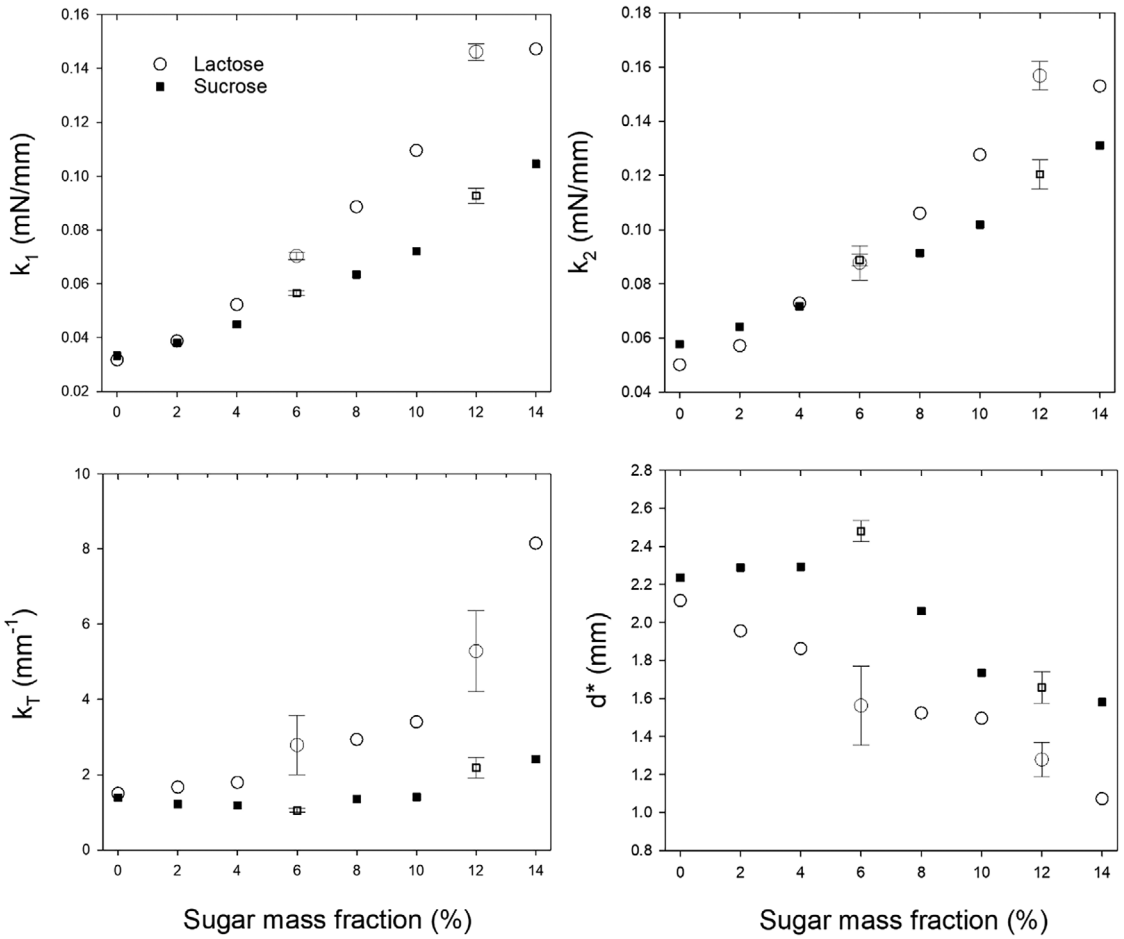


FIGURE 4 | Adjusted model parameters describing the elastic–plastic section of the force–displacement curves as a function of sugar concentration: (a) slope of the low-indentation region (k_1), (b) slope of the high-indentation region (k_2), (c) transition slope (k_T), and (d) characteristic indentation depth (d^*).

our system. The significantly stronger increases in slope of the lactose gels must therefore be explained by additional, lactose-specific mechanisms. It is more likely that the stronger effect of lactose is due to specific physical interactions, in particular hydrogen bonding between the hydrophilic protein segments and the hydroxyl groups of the sugar, as described, for example, by Vega and Roos to explain delays in sugar crystal growth [19].

The two parameters of the transition function (d^* and k_T) already differ between the two sugar types at low sugar concentrations. The steepness of the transition (k_T) increases slightly at first and then significantly more strongly with increasing sugar concentration, with the values for lactose always being higher than those for sucrose. In contrast, the values for the transition position (d^*) tend to decrease with increasing sugar concentration. Here, the values for sucrose gels are generally higher than those for lactose gels, although, in contrast to lactose gels, a pronounced decrease only occurs at concentrations above 6% sucrose. This indicates that gels produced with lactose form a denser and mechanically more homogeneous network. The stronger protein–protein interactions resulting from the dehydration of caseins make the gel strands stiffer and less deformable. This means that the network can be stretched less under load, and the transition from the reversible elastic to the irreversible (plastic) range occurs earlier and at lower penetration depths. Given the mild heating conditions used in this study (70°C for 11 min), the formation of significant Maillard reaction products is unlikely [29, 30]. Consequently, glycation reactions between lactose as a reducing sugar and caseins are not expected to be responsible for the observed effects of lactose or for the differences between lactose- and sucrose-containing systems. A similar trend toward a sharper and earlier onset of the transition function has also been described for gels in which free thiol groups on the micelle surface were blocked by N-ethylmaleimide (NEM), which also resulted in a more homogeneous and mechanically uniform network structure [27].

Model curves were calculated from the fit parameters and used as background functions for subtracting from the measured force–displacement curves. This makes the previously mentioned sugar peak clearer in terms of its shape and location (Figure 2), enabling a more detailed analysis below.

3.3 | Peak Isolation and Comparison

The sugar peak obtained in this way is shown in Figure 5a for lactose and in Figure 5b for sucrose.

25109936, 2026, 2, Downloaded from https://chemistry-europe.onlinelibrary.wiley.com/doi/10.1002/cfch.202500049 by Universitatsbibliothek RWTH Aachen University, Wiley Online Library on [10/06/2026]. See the Terms and Conditions (https://onlinelibrary.wiley.com/terms-and-conditions) on Wiley Online Library for rules of use; OA articles are governed by the applicable Creative Commons License

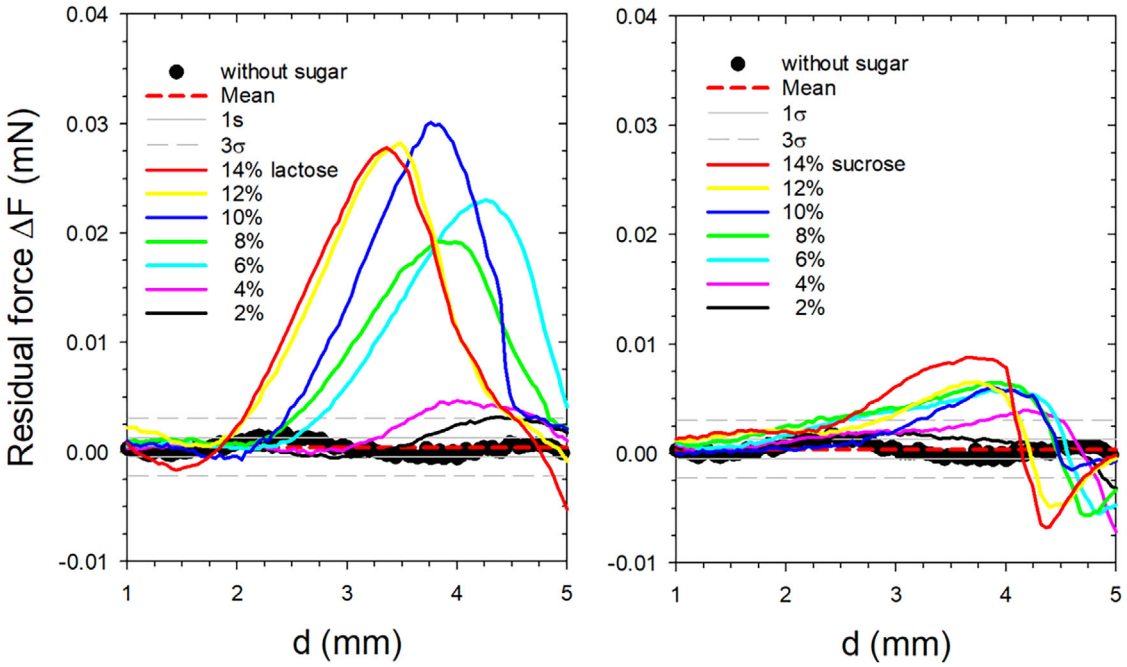


FIGURE 5 | Residual force curves of acidic MC–gels containing various amounts of lactose (a) and sucrose (b) as a function of penetration depth, compared to sugar-free reference measurements; ±1σ intervals derived from a model fit (Equations 1 and 3) to the reference data are shown as grey solid line. The 3σ threshold value (range indicated by dashed lines) is also shown across the entire penetration range. Measurements on samples containing more than 6% lactose exhibit clear peaks that significantly surpass the 3σ limit value.

The difference signal clearly exceeds the 3σ error limit derived from the model fit to the sugar-free force curve for both sugars. While pronounced sugar peaks become visible from a lactose addition of 6%, with maxima exceeding the 3-σ limit by a factor of about 10 (Figure 5a), the peaks caused by sucrose remain irregular in shape. They show a flat rising left flank and a steep falling right flank and reach maximum values in the range of three times the error limit (Figure 5b). The fact that the peak occurs independently of additional preheating of the solution to 70°C (data not shown) suggests that the structural conditions for subsequent interactions with lactose were already established in the powder matrix or during the previous thermal treatment of the powder. The increase in the force peak observed from 6% to 14% lactose can then be explained by the increasing cross-linking of the gel matrix. The stronger local sugar load would in turn lead to earlier bond overload and a partial breakage of the additional interactions, which is reflected in the peak shift from 4.2 to 3.2 mm. Although sucrose can also form hydrogen bonds [19], its specific structure and spatial fit in the gel could result in weaker whey protein-casein interactions, leaving the peak smaller and broader.

3.4 | System Dynamics Analysis of Sugar Peaks

To model the residual force peak, we performed a system dynamics analysis. This allowed us to record the chronological sequence of processes during the force peak, thereby separating the elastic material responses from the effects of relaxation of the gel network and the load limits of the sugar bonds. First, the residual force curve $F(x)$ is converted to $F(t) = F(x/v)$ at a constant penetration speed (v = 0.1 mm/s). The momentum transfer $p(t)$ from the indenter to the casein gel can then be calculated from this by numerical integration. Figure 6a shows the $p(t)$ curves for 12%, 8%, and 4% lactose as examples. As the lactose concentration increases, the curves begin at an earlier stage, rise more steeply and reach higher final values. This indicates that the resistance to indentation of the gel increases with sugar-induced network hardening, resulting in faster and greater momentum transfer from the indenter.

For system dynamics modeling, a linear force curve (dashed lines, Figure 6b) is used as the input function.

$$F_{\text{in}}(t) = k \cdot t \tag{4}$$

This approach is based on the assumption that the force peak is caused by sugar–reinforced bonds stretching like a linear spring with stiffness k. To activate the process, we use a first-order lagged pulse function, $u(t)$, which describes both the stress range of the sugar bonds and the relaxation effects of the gel network:

$$u(t) = \begin{cases} 0 & t < t_1 \\ 1 - e^{-\frac{t-t_1}{\tau}} & t_1 \le t \le t_2 \\ \left(1 - e^{-\frac{t_2-t_1}{\tau}}\right) \cdot e^{-\frac{t-t_2}{\tau}} & t > t_2 \end{cases} \tag{5}$$

where t_1 and t_2 describe the start and end times of peak formation, and τ is the characteristic time of the gel network.

The product of the pulse and linear force functions:

$$F_{\text{eff}}(t) = F_{\text{in}}(t) \cdot u(t) \tag{6}$$

25109936, 2026, 2, Downloaded from https://chemistry-europe.onlinelibrary.wiley.com/doi/10.1002/cfch.202500049 by Universitatsbibliothek RWTH Aachen University, Wiley Online Library on [10/06/2026]. See the Terms and Conditions (https://onlinelibrary.wiley.com/terms-and-conditions) on Wiley Online Library for rules of use; OA articles are governed by the applicable Creative Commons License

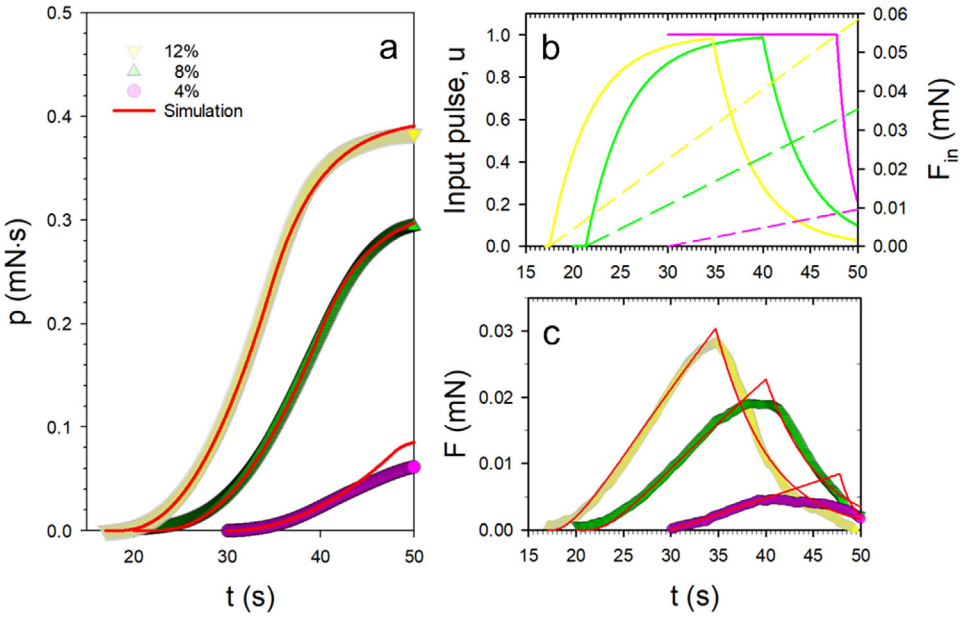


FIGURE 6 | System dynamics modeling of the residual force peak with 12%, 8% and 4% lactose: (a) The numerically integrated impulse $p(t)$ is compared with the simulation. (b) The input functions are the pulses $u(t)$ and the linear elastic force functions F_{in}. (c) The residual force peaks (residual force data) are compared with the modelled force curves F_{eff}.

TABLE 2 | Parameter values used for the simulation in Figure 6.

Parameter	4%	8%	12%	14%
k (mN·s^{-1})	0.0005	0.0012	0.0018	0.002
τ (s)	1.43	4.33	4.3	4.3
t_1 (s)	30	21.3	17.5	18.1
t_2 (s)	47.8	40	34.7	34.2

serves as the input function for momentum balance in the system dynamics model. The modeled momentum response can then be obtained by integrating this effective input via:

$$p_{mod}(t) = \int_0^t F_{eff}(t')\, dt' \quad (7)$$

and compared with the measured $p(t)$. The parameter values used for the simulations are summarized in Table 2.

As the system dynamics analysis in Figure 6 shows there is good agreement between the measurements (symbols) and the simulation results (red lines). This applies to both the transmitted pulse $p(t)$ (Figure 6a) and the residual force peak F_{eff} used as the model input (Figure 6c).

Figure 6b shows the corresponding pulse functions and linear force increases. As Table 2 shows, the slope k of the linear force function increases with lactose content (from 0.0005 mN s^{-1} at 4% to 0.002 mN s^{-1} at 14%), reflecting the trend toward steeper force peaks. With increasing lactose concentration, the pulse functions start at earlier times t_1 (from 30 to ≈ 18 s) and end earlier (t_2 from 47.8 s to ≈ 34 s). This shift to earlier pulse start times indicates that sugar-induced network hardening enables the gel to transmit the applied tension more quickly, resulting in faster force build-up.

The shape of the pulse function changes from an almost constant value (4%) to a characteristic, initially steep and then flattening curve (8% and 12%), indicating a stronger viscoelastic response of the gel network. In Figure 6c, this results in an increasingly steep and pronounced force peak. At 4% lactose, there is only a linear increase without a clear peak, at 8% there is a distinct but flattened peak, and at 12% there is almost complete agreement with the modeled curve. These trends correspond to the simulated impulse curves in Figure 6a, which show increasingly better agreement with the curves obtained from the measurements for higher lactose contents. The time constant τ is approximately 4.3 s for all conditions and describes the time-dependent viscous delay of the binding stress in the gel; only at 4% lactose is τ significantly lower at 1.43 s. The consistent value of τ for higher concentrations indicates a dominant viscous mechanism that determines the dynamic response of the gel during the build-up and decay of the force peak.

A corresponding model analysis of the sucrose-induced peaks (Figure 5b) is presented in the Figure S3 and Table S2. Compared to lactose, sucrose gels exhibit significantly lower force peaks and shorter relaxation times τ. Although the peaks are similarly broad, they reach only about one-third of the height and drop off abruptly because the weaker sugar–protein bonds build up less stress and break more quickly. As a result, the viscoelastic casein network stores stress only briefly, even at high sucrose concentrations.

4 | Conclusion

While no clear effect was apparent in the microstructure of the sucrose-containing gels compared to the sugar-free gel, the already known compacting influence of lactose on the microstructure was confirmed. It was newly discovered that this

25109936, 2026, 2, Downloaded from https://chemistry-europe.onlinelibrary.wiley.com/doi/10.1002/cfch.202500049 by Universitatsbibliothek RWTH Aachen University, Wiley Online Library on [10/06/2026]. See the Terms and Conditions (https://onlinelibrary.wiley.com/terms-and-conditions) on Wiley Online Library for rules of use; OA articles are governed by the applicable Creative Commons License

lactose-induced structural densification increases gel stiffness and leads to greater local force amplification, while a comparable but less pronounced peak is also visible in sucrose gels.

Force–displacement curves showed two consecutive linear regions whose slopes (k_1 and k_2) increased with increasing sugar concentration, indicating enhanced protein–protein interactions due to osmotic dehydration. The significantly stronger effects in lactose gels compared to sucrose gels indicate additional sugar-specific interactions, presumably mediated by hydrogen bonds between sugar hydroxyl groups and hydrophilic protein segments.

The sugar peak visible in the force curves was isolated by subtracting the modeled background curves, revealing differences in the shape and position of the residual peaks between lactose and sucrose gels. As the penetration rate remained constant, it was possible to transform the force curve into the time domain and calculate the impulse transferred to the gel. The resulting integrated impulse function was then modeled using system dynamics, with a linear force curve for the material stiffness of the gel and a delayed pulse for the temporal dynamics of the viscoelastic network reactions as input functions.

The time constant τ obtained from the simulation remained at around 4.3 s even at higher lactose concentrations, suggesting that the viscous, time-dependent processes of the network remain largely unchanged. τ represents the characteristic reaction time of the gel network, which determines both the delayed stress buildup and the subsequent relaxation of the sugar-reinforced bonds. It arises from rearrangements of noncovalent casein–casein contacts, segmental mobility of the casein strands, and local viscous dissipation of water and polymer segments. The nearly constant τ therefore shows that lactose mainly increases the elastic coupling within the network via stronger or more numerous protein contacts without significantly altering the intrinsic dynamics of bond rearrangement or local viscous damping, which would otherwise modify this time scale. The earlier and more pronounced peaks at higher lactose concentrations can be attributed to the accelerated stress buildup and premature failure of the bonds stiffened by lactose. These peaks also serve as mechanical probes that can be used to assess the viscoelastic behavior of the gel in indentation tests. In contrast, sucrose gels exhibit smaller and less pronounced peaks as well as significantly shorter relaxation times, suggesting lower stress buildup and reduced viscoelastic coupling to the casein network.

Acknowledgments

We thank Alexandra Airich and Marie Schmitt for their support with the experiments. This work was supported by the Confocal Microscopy Facility of the Interdisciplinary Center for Clinical Research (IZKF) within the Faculty of Medicine at RWTH Aachen University. We are also grateful to MILEI GmbH for the generous provision of the micellar casein powder.

Conflicts of Interest

The authors declare no conflicts of interest.

Data Availability Statement

The data that support the findings of this study are available from the corresponding author upon reasonable request.

References

1. Y. Cao and R. Mezzenga, "Design Principles of Food Gels," *Nature Food* 1 (2020): 106–118, https://doi.org/10.1038/s43016-019-0009-x.

2. A. Foroutan, A. C. Guo, R. Vazquez-Fresno, et al., "Chemical Composition of Commercial Cow's Milk," *Journal of Agricultural and Food Chemistry* 67 (2019): 4897–4914, https://doi.org/10.1021/acs.jafc.9b00204.

3. R. Bouma, E. Bijl, A. Thiel, and K. Hettinga, "Comparing Coagulation Behaviour of Reassembled and Native Casein Micelles During Renneting, Acid Gelation and Gastric Clotting," *Food Hydrocolloids* 168 (2025): 111441, https://doi.org/10.1016/j.foodhyd.2025.111441.

4. S. Thill, T. Schmidt, S. Jana, D. Wöll, and R. Gebhardt, "Fine Structure and Swelling Properties of Fibers From Regenerated Rennet-Treated Casein Micelles," *Macromolecular Materials and Engineering* 307 (2022): 2200272, https://doi.org/10.1002/mame.202200272.

5. P. E. AcuñaAvila, S. CortesCamargo, and A. JiménezRosales, "Properties of Micro and Nano Casein Capsules Used to Protect the Active Components: A Review," *International Journal of Food Properties* 24 (2021): 1132–1147, https://doi.org/10.1080/10942912.2021.1953069.

6. C. G. De Kruif, T. Huppertz, V. S. Urban, and A. V. Petukhov, "Casein Micelles and Their Internal Structure," *Advances in Colloid and Interface Science* 171-172 (2012): 36–52, https://doi.org/10.1016/j.cis.2012.01.002.

7. J. P. Hindmarsh and P. Watkinson, "Experimental Evidence for Previously Unclassified Calcium Phosphate Structures in the Casein Micelle," *Journal of Dairy Science* 100 (2017): 6938–6948, https://doi.org/10.3168/jds.2017-12623.

8. R. Gebhardt, N. Takeda, U. Kulozik, and W. Doster, "Structure and Stabilizing Interactions of Casein Micelles Probed by High-Pressure Light Scattering and FTIR," *Journal of Physical Chemistry B* 115 (2011): 2349–2359, https://doi.org/10.1021/jp107622d.

9. C. G. De Kruif and E. B. Zhulina, "κ-Casein as a Polyelectrolyte Brush on the Surface of Casein Micelles," *Colloids and Surfaces A: Physicochemical and Engineering Aspects* 117 (1996): 151–159, https://doi.org/10.1016/0927-7757(96)03696-5.

10. R. Tuinier and C. G. De Kruif, "Stability of Casein Micelles in Milk," *Journal of Chemical Physics* 117 (2002): 1290–1295, https://doi.org/10.1063/1.1484379.

11. J. A. Lucey, D. J. Wilbanks, and D. S. Horne, "Impact of Heat Treatment of Milk on Acid Gelation," *International Dairy Journal* 125 (2022): 105222, https://doi.org/10.1016/j.idairyj.2021.105222.

12. T. P. Guinee, B. T. O'Kennedy, and P. M. Kelly, "Effect of Milk Protein Standardization Using Different Methods on the Composition and Yields of Cheddar Cheese," *Journal of Dairy Science* 89 (2006): 468–482, https://doi.org/10.3168/jds.S0022-0302(06)72110-5.

13. M. Warncke, "Functionality of MC88- and MPC85-Enriched Skim Milk: Impact of Shear Conditions in Rotor/Stator Systems and High-Pressure Homogenizers on Powder Solubility and Rennet Gelation Behavior," *Foods* 10 (2021): 1361, https://doi.org/10.3390/foods10061361.

14. R. Gebhardt, C. Hohn, and M. Asaduzzaman, "Stabilizing Interactions of Casein Microparticles After a Thermal Post-Treatment," *Food Chemistry* 450 (2024): 139369, https://doi.org/10.1016/j.foodchem.2024.139369.

15. R. Gebhardt and C. Hohn, "Kinetic Description of Changes in the Size of Casein Microparticles Under Simulated Gastric Conditions," *Scientific Reports* 15 (2025): 35406, https://doi.org/10.1038/s41598-025-22216-7.

16. C. Bastard, J. C. T. Schulte, M. Asaduzzaman, et al., "Casein Microparticles Filled With Cellulase to Enzymatically Degrade Nanocellulose for Cell Growth," *Biomaterials Science* 13 (2025): 2435–2443, https://doi.org/10.1039/D4BM01508H.

25109936, 2026, 2, Downloaded from https://chemistry-europe.onlinelibrary.wiley.com/doi/10.1002/cfch.202500049 by Universitatsbibliothek RWTH Aachen University, Wiley Online Library on [10/06/2026]. See the Terms and Conditions (https://onlinelibrary.wiley.com/terms-and-conditions) on Wiley Online Library for rules of use; OA articles are governed by the applicable Creative Commons License

17. M. G. Semenova, A. S. Antipova, and L. E. Belyakova, "Food Protein Interactions in Sugar Solutions," *Current Opinion in Colloid & Interface Science* 7, no. 5-6 (2002): 438–444, https://doi.org/10.1016/S1359-0294(02)00079-1.

18. Y. I. Sánchez-García, N. Gutiérrez-Méndez, R. E. Orozco-Mena, V. H. Ramos-Sánchez, and M. Y. Leal-Ramos, "Individual and Combined Effect of pH and Whey Proteins on Lactose Crystallization," *Food Research International* 116 (2019): 455–461, https://doi.org/10.1016/j.foodres.2018.08.061.

19. C. Vega and Y. H. Roos, "The State of Aggregation of Casein Affects the Storage Stability of Amorphous Sucrose, Lactose, and Their Mixtures," *Food Biophysics* 2, no. 1 (2007): 10–19, https://doi.org/10.1007/s11483-007-9024-9.

20. S. M. Mozersky, H. M. Farrell Jr, and R. A. Barford, "The Effects of Sucrose and Lactose on the Sizes of Casein Micelles Reconstituted From Bovine Caseins," *Journal of Dairy Science* 74, no. 8 (1991): 2382–2393, https://doi.org/10.3168/jds.S0022-0302(91)78412-9.

21. L. E. Belyakova, A. S. Antipova, M. G. Semenova, E. Dickinson, L. M. Merino, and E. N. Tsapkina, "Effect of Sucrose on Molecular and Interaction Parameters of Sodium Caseinate in Aqueous Solution: Relationship to Protein Gelation," *Colloids and Surfaces B: Biointerfaces* 31 (2003): 31–46, https://doi.org/10.1016/S0927-7765(03)00041-9.

22. L. A. Pugnaloni, L. Matia-Merino, and E. Dickinson, "Microstructure of Acid-Induced Caseinate Gels Containing Sucrose: Quantification From Confocal Microscopy and Image Analysis," *Colloids and Surfaces B: Biointerfaces* 42 (2005): 211–217, https://doi.org/10.1016/j.colsurfb.2005.03.002.

23. G. H. Meletharayil, H. A. Patel, L. E. Metzger, and T. Huppertz, "Acid Gelation of Reconstituted Milk Protein Concentrate Suspensions: Influence of Lactose Addition," *International Dairy Journal* 61 (2016): 107–113, https://doi.org/10.1016/j.idairyj.2016.04.005.

24. J. Mazurkiewicz and M. Nowotny-Różańska, "Viscosity of Aqueous Solutions of Saccharides," *Polish Journal of Food and Nutrition Sciences* 48, no. 2 (1998): 171–180.

25. P. Lemke, S. Moench, P. S. Jäger, et al., "Micromechanical Indentation Platform for Rapid Analysis of Viscoelastic Biomolecular Hydrogels," *Small Methods* 8, no. 12 (2024): 2400251, https://doi.org/10.1002/smtd.202400251.

26. M. Rief, M. Gautel, F. Oesterhelt, J. M. Fernandez, and H. E. Gaub, "Reversible Unfolding of Individual Titin Immunoglobulin Domains by AFM," *Science* 276 (1997): 1109–1112, https://doi.org/10.1126/science.276.5315.1109.

27. T. Pütz and R. Gebhardt, "Tuning the Gel Network Structure and Rheology of Acid-Induced Casein Gels via Thiol Blocking," *International Journal of Molecular Sciences* 26, no. 13 (2025): 6206, https://doi.org/10.3390/ijms26136206.

28. J. Dumpler, "Preparation of simulated milk ultrafiltrate," in *Heat Stability of Concentrated Milk Systems*, (Springer Spektrum, 2018), https://doi.org/10.1007/978-3-658-19696-7_6.

29. F. J. Morales and M. A. J. S. Van Boekel, "A Study on Advanced Maillard Reaction in Heated Casein/Sugar Solutions," *International Dairy Journal* 7, no. 11 (1997): 675–683, https://doi.org/10.1016/S0958-6946(97)00071-X.

30. M. A. J. S. Van Boekel, "Effect of Heating on Maillard Reactions in Milk," *Food Chemistry* 62, no. 4 (1998): 403–414, https://doi.org/10.1016/S0308-8146(98)00075-2.

Supporting Information

Additional supporting information can be found online in the Supporting Information section.

Supplementary File 1: cfch70013-sup-0001-SuppMat.pdf.

25109936, 2026, 2, Downloaded from https://chemistry-europe.onlinelibrary.wiley.com/doi/10.1002/cfch.202500049 by Universitatsbibliothek RWTH Aachen University, Wiley Online Library on [10/06/2026]. See the Terms and Conditions (https://onlinelibrary.wiley.com/terms-and-conditions) on Wiley Online Library for rules of use; OA articles are governed by the applicable Creative Commons License